Spontaneous oscillations of a sessile lens

ROMAN STOCKER[1] AND JOHN W. M. BUSH[2]

[1]Ralph M. Parsons Laboratory, Department of Civil and Environmental Engineering,
MIT, Cambridge, MA, USA
romans@mit.edu

[2]Department of Mathematics, MIT, Cambridge, MA, USA
bush@math.mit.edu

When an oil drop is placed on a water surface, it assumes the form of a sessile lens. We consider the curious behaviour that may arise when the oil contains a water-insoluble surfactant: the lens radius oscillates in a quasi-periodic fashion. While this oscillatory behaviour has been reported elsewhere, a consistent physical explanation has yet to be given. We present the results of an experimental investigation that enable us to elucidate the subtle mechanism responsible. Videomicroscopy reveals that the beating behaviour is generated by a subtle process of partial emulsification at the lens edge and sustained by evaporation of surfactant from the water surface.

1. Introduction

We examine a peculiar process of spontaneous oscillations exhibited by a drop of mineral oil containing oil-soluble surfactant and placed on a water surface as a sessile lens. Within a range of surfactant concentrations, the lens executes a quasi-periodic beating pattern that manifests itself as oscillations of the lens radius, and can persist for an extended period, on the order of an hour. Figure 1(a, b) shows two sample time series of the lens radius. A composite picture of the lens in its states of maximum expansion and contraction is shown in figure 2(a). This phenomenon was reported and described qualitatively by Sebba (1975); however, no quantitative experimental study was undertaken and no consistent physical mechanism proposed.

The spreading of an oil lens on the surface of water is a topic of long-standing interest (Franklin 1774). The dynamics of the lens can be described in terms of the spreading coefficient $S = \sigma_{wa} - \sigma_{oa} - \sigma_{ow}$, which gives the balance between the interfacial tensions at the oil–water–air triple junction. Here σ_{wa}, σ_{oa}, and σ_{ow} are the interfacial tensions between air and water, oil and air, and oil and water, respectively. For $S > 0$, the droplet spreads to a layer of molecular thickness (e.g. Foda & Cox 1980). For $S < 0$, an equilibrium configuration arises and the drop assumes the form of a sessile lens. The statics (Pujado & Scriven 1972) and dynamics (Miksis & Vanden-Broeck 2001) of a sessile lens are well-studied. Here we describe a configuration for which no equilibrium shape emerges: the spreading coefficient is time-dependent and the lens characterized by quasi-periodic oscillations in radius.

Previous work on spontaneous oscillations has largely been motivated by a desire to find physicochemical analogues to biological and physiological systems. This perspective was summarized by Sebba (1979): "The ultimate goal of physiologists is to be able to explain living behaviour in terms of physicochemical forces. Thus, any expansion of our knowledge of such forces, based on inanimate systems, should
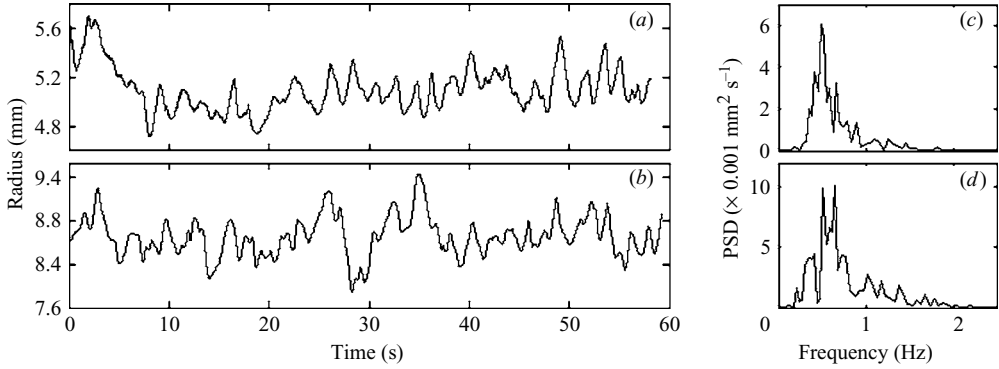
FIGURE 1. The time evolution of the lens radius for 10 % Tergitol concentration, for two lens volumes: (*a*) 25 μl; (*b*) 100 μl. The associated power spectral densities are given in (*c*) and (*d*).
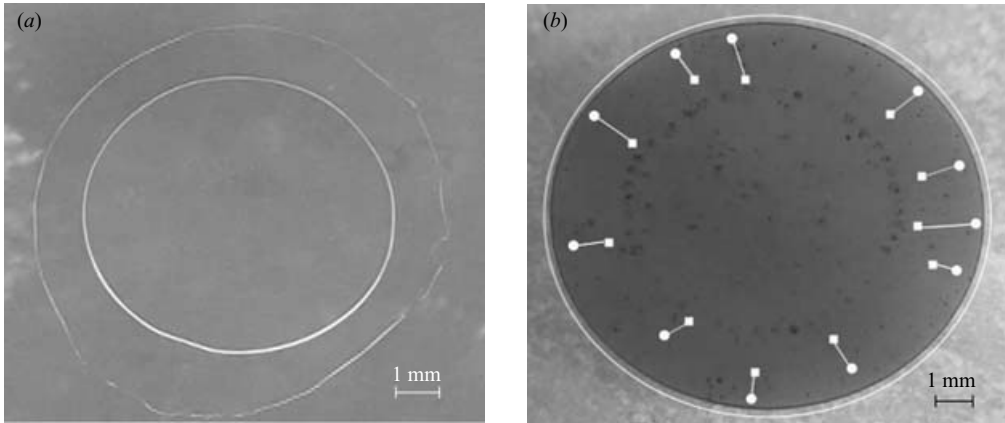

FIGURE 2. (*a*) A lens at its stages of maximum expansion and contraction. The image was obtained by superposing two frames of a video sequence. (*b*) Particle tracking within the lens. Shown in white are particle tracks on the upper lens surface obtained over 5 s. Circles and squares indicate starting and ending points, respectively. The circulation is radially inwards and outwards on, respectively, the upper and lower lens surface. The dark ring of particles indicates the limited radial extent of the circulation. The white outline indicates the maximum lens radius.

be examined to see whether this might not offer insight into biological behaviour". Spontaneous oscillations arise in a wide variety of natural systems, including nerve cells and muscle tissue, mitochondria, and biological clocks such as those responsible for circadian rhythms (Goldbeter 1996).

Spontaneous oscillations in fluid systems typically arise as a result of the conversion of one form of energy into another, often chemical into kinetic energy. Such oscillations have been reported in a variety of systems and are particularly striking when the source of energy is not readily apparent. One such example is the 'spitting drop' (Fernandez & Homsy 2004; Krechetnikov & Homsy 2004) which arises when a pendant drop of water is immersed in oil. Both oil and water phases contain solutes that react to produce a surfactant at the drop interface. The non-uniform distribution of surfactant on the drop surface results in a surface tension gradient that drives a Marangoni flow (Scriven & Sternling 1960) that transports surfactant

to the tip of the drop, from which it is ejected into the surrounding oil in a manner reminiscent of tip-streaming (Taylor 1934). Other forms of spontaneous oscillations have been reported that do not prompt interfacial deformation, but may be measured as quasi-periodic variations in surface tension, pH or electric potential (e.g. Dupeyrat & Nakache 1978; Yoshikawa & Matsubara 1983; Kovalchuk *et al.* 1999; Shioi *et al.* 2002).

Sebba & Briscoe (1940) reported spontaneous oscillations of a sessile lens of cetyl alcohol on water. The lens contracts and expands with a characteristic period of several minutes. They rationalized the contraction phase as being due to the transfer of surfactant from the lens to the water surface. Two mechanisms for the expansion phase were considered: evaporation of alcohol, and its dissolution into the water, both of which lead to an increase of the water surface tension. They opted for the dissolution mechanism because "it seems very improbable that a heavy molecule [i.e. cetyl alcohol] of such high boiling point should be readily volatile". They do note, however, that other substances of high boiling point may evaporate when spread on water.

Sebba (1975) reported oscillations in the radius of an oil lens mixed with Tergitol, the oil-soluble surfactant to be considered in our study. Sebba (1975) did not investigate these oscillations in any detail, nor did he quantify the period of oscillation. Rather, he claimed that the mechanism responsible was analogous to that considered in Sebba & Briscoe (1940): adsorption of surfactant at the lower lens interface drives expansion, while dissolution of surfactant into the underlying water causes contraction. We here report new observations of this system that yield insight into its rich dynamics. In particular, we demonstrate that the critical mechanism responsible for the oscillations is the ejection of surfactant onto the free surface via partial emulsification at the lens edge. We further demonstrate that evaporation of surfactant from the water surface plays a critical role in sustaining the oscillations.

2. Experimental method

Oscillations of a sessile lens can be observed by placing a drop of oil mixed with oil-soluble surfactant on a water surface. We used commercially available mineral oil (Cumberland Swan, density $873\,\mathrm{kg\,m^{-3}}$, dynamic viscosity $0.157\,\mathrm{kg\,m^{-1}\,s^{-1}}$ at $25\,^{\circ}\mathrm{C}$). The oil-soluble surfactant was Tergitol 15-S-3 (Dow Corning, density $918\,\mathrm{kg\,m^{-3}}$, dynamic viscosity $0.026\,\mathrm{kg\,m^{-1}\,s^{-1}}$ at $25\,^{\circ}\mathrm{C}$), a secondary alcohol ethoxylate. Tergitol is a non-ionic surfactant, insoluble in water. A given fraction of the surfactant (typically 10 % by weight) was mixed with the oil by gentle stirring. The mixture could be used for several weeks after preparation, but had to be stirred before use as the heavier Tergitol settles out of solution over a time scale of several hours.

A clean Petri dish (diameter 8 cm) was filled to a depth of 4 mm with deionized water and left to relax until residual circulations dissipated. Experiments with tap water gave irreproducible results, attesting to the importance of a clean water surface. A sessile lens was created by gently placing a given volume of the oil–surfactant mixture onto the surface of the water at the approximate centre of the Petri dish using a pipette. A series of 41 experiments was performed by varying the lens volume (between 25 and $400\,\mu\mathrm{l}$) and surfactant concentration. The surfactant concentration was varied between 4 % and 25 %: outside this range, only sporadic beating was observed. To quantify the amplitude and period of the spontaneous oscillations, the dish was placed on a ring stand and lit from below by a fibre-optic light source, whose presence did not affect the lens behaviour. Black paper placed beneath the Petri dish

provided maximum contrast between the almost transparent lens and the water. The oscillations were captured at $30\,\mathrm{frame\,s}^{-1}$ with a Sony TRV950 digital videocamera mounted vertically above the lens. Before each experiment, a calibration image was taken using graph paper. To characterize the evolution of the lens radius, videos were analysed in *Matlab*: each image was thresholded to determine the lens edge and the lens radius was computed from the number of pixels within the lens. The accuracy of this edge tracking algorithm was tested by comparing the inferred and actual lens edges over a range of frames. From the time series of the lens radius, the power spectral density (PSD) was calculated using the fast Fourier transform in *Matlab*, with time-domain averaging and a cosine taper window. Additional experiments were carried out in order to visualize the circulation within the lens, by adding small particles (e.g. dust) to the oil–Tergitol mixture. Finally, the stability of the lens edge was examined at $20\,\mathrm{frame\,s}^{-1}$ using a Phantom V5.1 digital videocamera mounted on a compound microscope (Zeiss Axioskop 2) with a 10X objective.

3. Observations

A series of experiments was performed in order to delineate the range of conditions over which periodic oscillations arose. Beating was seen to be independent of container shape (round or square) and size (50–300 mm diameter or length), as well as layer depth (2–110 mm) over the range of lens volumes (25–400 μl) considered. A lens made of mineral oil and Triton (10 %) was readily observed to beat, while using dodecanol (10 % to 20 %) as the surfactant suppressed the beating. No lens was obtained by using hexadecane and Tergitol (10 %), which completely emulsified on the water surface. Adding glycerol to the water (up to 50 % by weight) did not suppress the beating; the same is true for small amounts of Oil Red dye (Sigma-Aldrich) added to the lens, which improved visualization. The most robust beating arose with 2 % to 30 % Tergitol in mineral oil, the system to be detailed in what follows.

The lens exhibits rich dynamics that depend on both time and initial surfactant concentration. When the drop first comes into contact with the water surface, it expands radially, and its edge bursts via a series of small eruptions. These eruption events correspond to spontaneous emulsification of the lens, prompted by the large initial difference between σ_{wa} and σ_{ow}. This eruption stage lasts a few seconds, after which the water surface is covered with myriad 100 μm-scale oil–surfactant droplets, which Sebba (1979) refers to as aphrons. Following partial emulsification, large lenses settle into a quasi-periodic beating state. Smaller lenses may be completely consumed by this initial emulsification process. However, when a new lens is placed on the water surface (now covered in surfactant), it starts beating. The need to 'sacrifice' the first lens to observe beating of subsequent lenses was pointed out by Sebba (1975). We note that, due to the highly irregular nature of the emulsification, the lens may drift off-centre and eventually attach to the container wall. The longest beating sequence we observed was 25 minutes. Data were acquired only while a lens was centred in the Petri dish. During the oscillations, the lens edge was predominantly smooth, but the contraction phase was preceded by a slight wrinkling of the edge visible to the naked eye and apparent in figure 2(*a*).

The radius of the beating lens was tracked as a function of time and the results are summarized in table 1. A measure of the amplitude of the spontaneous oscillations is $\sigma_r/\bar{r}$, where σ_r is the standard deviation of the lens radius over time, and $\bar{r}$ is the mean lens radius. The mean amplitude is typically 4 % of the lens radius. The average speed of contraction was slightly larger than that of expansion: their ratio

Volume (μl)	25	100	400	100	100
Surfactant (%)	10	10	10	4	25
Runs	9	8	8	8	8
Total time (s)	376	354	477	394	312
Mean radius $\bar{r}$ (mm)	4.4 ± 0.2	8.1 ± 0.2	14.3 ± 0.4	8.1 ± 0.4	7.4 ± 0.2
Amplitude $\sigma_r/\bar{r}$ (%)	4.5 ± 0.3	4.1 ± 0.3	1.5 ± 0.3	3.1 ± 0.3	4.0 ± 0.3
CE	1.15 ± 0.03	1.13 ± 0.03	1.03 ± 0.01	1.13 ± 0.05	1.28 ± 0.05
Dominant period (s)	1.9 ± 1.4	1.8 ± 0.8	2.3 ± 0.7	2.6 ± 0.9	1.5 ± 0.7

TABLE 1. Summary of experimental runs. CE is the ratio of average speeds of contraction and expansion. Values have been averaged over all runs in each column, with each run weighted by its duration. The dominant period is the largest peak in the PSD (see figure 1c, d).

(CE) is in the range 1.03–1.28, indicating that the asymmetry is not pronounced. No clear correlation was evident between the amplitude of oscillation and either the lens volume or the surfactant concentration, but there is some indication that lenses with lower surfactant concentration oscillate more slowly.

Figure 1 illustrates that the oscillations, though robust, are not purely periodic. Table 1 shows that the dominant period is around 2 s, independent of the lens volume in the range examined. The considerable variability in period indicated by the large standard deviations presumably results from the sensitivity of the lens to inhomogeneities in surfactant distribution, as may arise from incomplete mixing of the lens fluid.

As the lens expands and contracts, the liquid inside circulates. Particle tracking revealed two interesting features (figure 2b). First, the circulation is radially inwards on the upper lens surface and outwards near the lower, with a characteristic speed of $1 \, \mathrm{mm \, s^{-1}}$. Second, the circulation is limited to the outer annulus of the lens, as revealed by the ring of particles in figure 2(b). Particles are advected radially inwards on the upper surface and accumulate at the point of downwelling, marking the edge of the circulation region. These observations concerning the direction and radial extent of the circulation will be important in rationalizing the oscillations.

One further observation proves crucial for understanding the mechanism. When a lid is placed on a Petri dish containing a pulsating lens, the oscillations stop immediately and the lens relaxes to a radius of maximum expansion. When the lid is removed, a sudden and violent lens contraction ensues, followed by resumed, regular beating. Finally, we note that the smell of Tergitol always accompanied the beating. These observations suggest the importance of evaporation of surfactant to the beating mechanism.

We proceed by examining the details of the instability of the lens edge. In particular, we report new observations indicating that Tergitol is advected along the oil–water interface and ejected onto the water surface via a flushing event. Videomicroscopy reveals that the contraction events are triggered by eruptions at the drop edges. In figure 3(a) one may observe a sheet of oil and Tergitol being shed from the lens onto the water surface in the form of a thin film enclosed by a rim. Two small droplets are visible, suggesting that the rim is undergoing a Rayleigh–Plateau instability. Figure 3(b) illustrates a later stage in an ejection event: the sheet has spread further, the thin film has ruptured and been sucked into the rim or lens. The capillary instability of the rim has now produced four visible droplets. The droplets, which eventually break loose and disperse on the water surface, correspond to Sebba's aphrons. These eruptions occur on a time scale of a few tenths of a second. Macroscopically, these
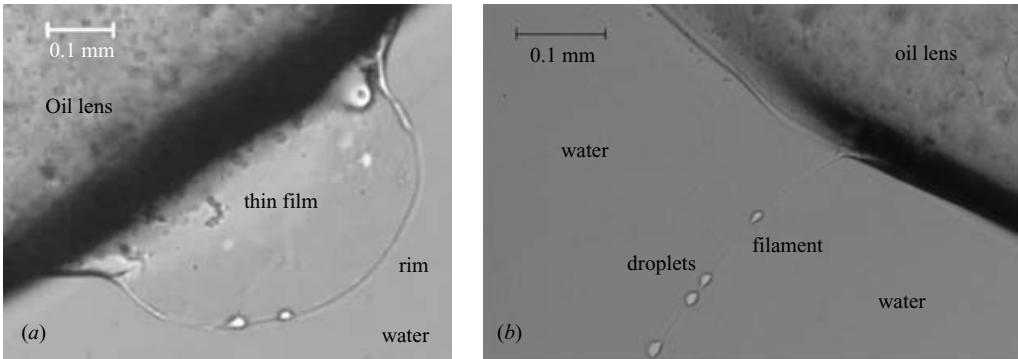
FIGURE 3. Ejection events. (*a*) A sheet of oil and surfactant is ejected from the lens onto the water surface, as revealed by the reflections. The sheet rim has begun to break into droplets. (*b*) A rim detaches from the lens and breaks into droplets. Ejection events occur over a few tenths of a second.
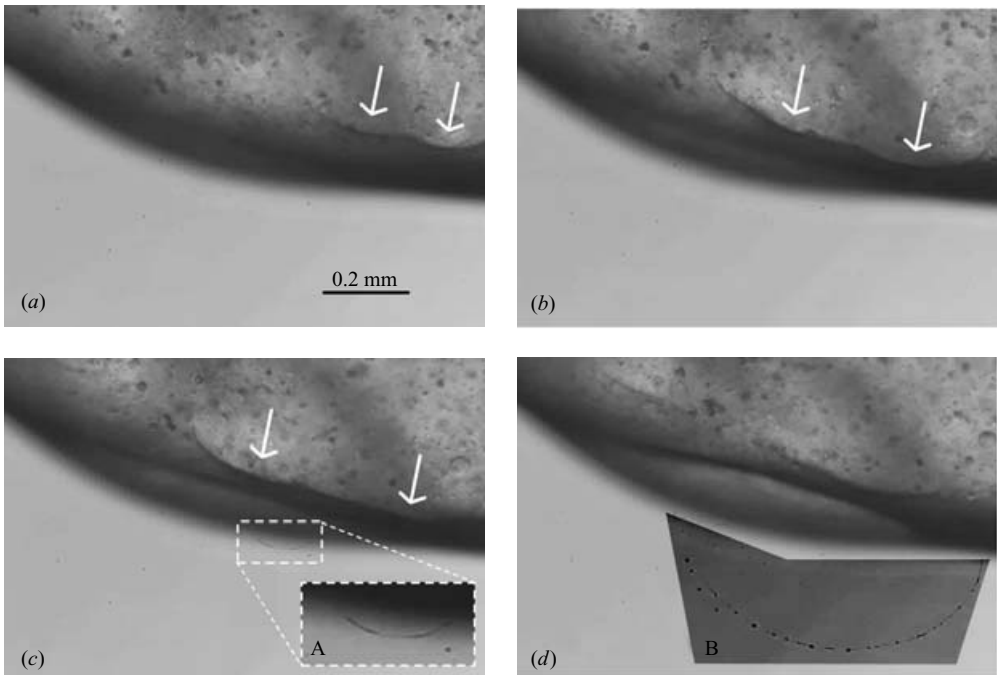

FIGURE 4. Details of an ejection event. The white arrows indicate the wave fronts moving radially outward (*a*, *b*, *c*) and breaking through the lens edge (*c*, *d*), ejecting oil and surfactant onto the water surface. The ejected sheet (shown in the boxed region in (*c*) and magnified in inset A with increased contrast), grows and breaks into droplets. The latter are evident in (*d*), where contrast has been enhanced in the polygonal area B to highlight the ejected material. Time between successive frames is 0.1 s.

microscopic eruptions correspond to the previously mentioned wrinkling of the lens edge evident in figure 2(*a*).

The details of the process leading to an eruption are difficult to observe as they occur at the lower interface of the lens; however, videomicroscopy did shed light on this process (figure 4). Two curved wave fronts propagating radially outwards along
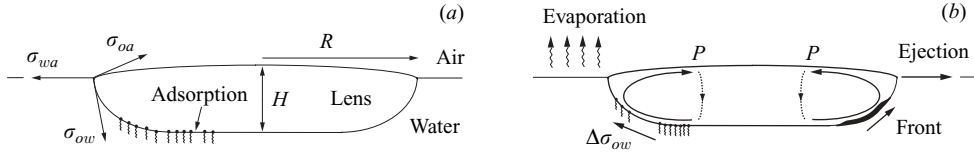
FIGURE 5. Schematic of the processes driving the oscillating lens. (*a*) Adsorption of the oil-soluble surfactant onto the lens–water interface reduces σ_{ow} and evaporation of surfactant from the water surface increases σ_{wa}, causing the lens to expand. (*b*) Differential adsorption generates a radial surface tension gradient $\Delta\sigma_{ow}$ that drives a circulation in the outer annulus of the lens (see figure 2*b*). The lower surface of the lens becomes unstable to a series of radially propagating waves that sweep surfactant onto the water surface, reducing σ_{wa} and causing the lens to contract.

the lower lens surface are visible in figure 4(*a*) (white arrows). Figure 4(*b*) shows that the fronts move from the interior of the lens towards its edge. In figure 4(*c*) the fronts have begun pushing a sheet of oil and Tergitol onto the water surface: this sheet is like that in figure 3(*a*), but here only the rim is visible. In figure 4(*d*) the sheet has ruptured, and the rim has broken up into droplets.

4. The mechanism

For a lens at rest, the three interfacial tensions σ_{wa}, σ_{oa}, and σ_{ow} (figure 5*a*) are in balance. Tergitol molecules in the oil lens adsorb at the lens interfaces (figure 5*a*), with a preference for the oil–water interface, since the surfactant tails are hydrophilic. Adsorption at the oil–water interface reduces σ_{ow}, causing the lens to expand. Since the lens is thinner at its edge, eventually the concentration of Tergitol molecules available for adsorption will be larger in the central region of the lens than at its edges. The resulting negative radial concentration gradient generates a positive radial interfacial tension gradient, thus a Marangoni stress directed radially outwards along the lower interface of the lens. This stress drives a circulation that is radially outwards near the lower interface, and therefore radially inwards near the upper interface, by continuity. The direction of this circulation is consistent with that observed (figure 2*b*). Since the surface tension gradient is anticipated only in a region near the edges, the circulation is expected only in the outer annulus of the lens, over a width of the order of the capillary length based on σ_{ow}, $l_c \sim [\sigma_{ow}/(g\,\Delta\rho)]^{1/2}$, where $\Delta\rho$ is the density contrast between the lens and water. For a typical lens, $l_c \sim 5$ mm is of the same order as the observed horizontal extent of the recirculation region (figure 2*b*).

Adsorption of surfactant onto the lower lens surface thus drives both the expansion of and circulation within the lens. To obtain oscillations, however, a restorative process is required to prompt the lens contraction. We first considered the possibility that Tergitol migrates directly from the oil–water interface into the bulk of the water, as suggested by Sebba & Briscoe (1940) for a cetyl alcohol lens and by Sebba (1975) for the system at hand. We ruled out this mechanism on the grounds that Tergitol is insoluble in water and is a non-ionic surfactant, a conclusion supported by the fact that the oscillations are unaffected by the water depth. Instead, we note that the eruptions detailed in figures 3 and 4 adequately account for the contraction phase: as Tergitol moves from the oil–water to the air–water interface, σ_{ow} increases and σ_{wa} decreases, and the lens contracts.

The proposed beating mechanism remains incomplete in that it does not provide a means by which the system reinitializes, without which the oscillations would cease

owing to the water surface becoming saturated in surfactant. The strong odour of Tergitol, together with the observation that beating stops as soon as a lid is placed on the Petri dish, suggest that evaporation of Tergitol is important. We confirmed that Tergitol can indeed evaporate by measuring the weight of a layer of pure Tergitol in a Petri dish over time, and found an evaporation rate of $Q = 4.3 \times 10^{-7}\,\mathrm{kg\,m^{-2}\,s^{-1}}$ at $20\,^{\circ}\mathrm{C}$. Evaporation thus reduces the Tergitol concentration on the water surface, thereby reinitializing the system. Note that evaporation also raises σ_{wa}, thus contributing to the growth of the lens radius in the expansion phase.

This physical picture suggests that the period of oscillation should correspond to the time scale of evaporation of Tergitol. If a mass M of surfactant is released onto the water surface after an ejection event, the surfactant rapidly spreads over an area A to a layer of molecular thickness h. The characteristic e-folding time for evaporation of surfactant is therefore $t_E \sim M/(QA) = \rho_S Ah/(QA) = \rho_S h/Q$, where ρ_S is the density of the surfactant. For our system, using a monolayer thickness $h = 2.1\,\mathrm{nm}$ corresponding to an 18-carbon chain at $0.125\,\mathrm{nm/carbon}$ bond (Mitchell *et al.* 1983), we obtain $t_E \sim 4.5\,\mathrm{s}$, comparable to the observed period of oscillation (table 1). We note that this scaling is consistent with the observed independence of oscillation period on container size. It is also consistent with the dependence of oscillation period on evaporation rate, as verified in experiments performed at a higher temperature. At $37\,^{\circ}\mathrm{C}$, the measured evaporation rate of tergitol was 2.2 times that at $20\,^{\circ}\mathrm{C}$. The beating period of a $10\,\%$ tergitol, $100\,\mu\mathrm{l}$ lens was found to be $0.9 \pm 0.4\,\mathrm{s}$, approximately half that at $20\,^{\circ}\mathrm{C}$ (see table 1). This variation is consistent with the predicted dependence $t_E \sim Q^{-1}$, and underscores the importance of evaporation of surfactant to the oscillations.

The final piece of the puzzle is rationalizing the eruption events shown in figures 3 and 4. We first considered the capillary instability of a two-layer system destabilized by a surfactant concentration gradient (Smith & Davis 1983). While this does represent a plausible mechanism in our parameter regime, these instabilities are not associated with interfacial distortions. Instead, we propose that the ejection events are prompted by the instability of a two-layer system due to the simultaneous presence of shear and interfacial surfactant (Frenkel & Halpern 2002; Halpern & Frenkel 2003; Blyth & Pozrikidis 2004; Frenkel & Halpern 2005). This insoluble-surfactant instability takes the form of interfacial waves and occurs even in the absence of inertia, provided $m < n^2$, where $m = \mu_2/\mu_1$, $n = d_2/d_1$, and μ_1 and d_1 are the dynamic viscosity and thickness of the upper layer, respectively, while μ_2 and d_2 are those of the lower layer.

This configuration is analogous to the case at hand, where the lens represents the upper layer, and the water the lower layer. Surfactant is brought to the interface by adsorption, and interfacial shear is generated by differential adsorption associated with the corner geometry, providing the necessary ingredients for instability of the lower lens interface. As the viscosity ratio m (=0.007) is always much smaller than the square of the layer thickness ratio n (>1) in our experiments, the lens–water interface is indeed expected to be unstable according to the criterion of Frenkel & Halpern (2002). We should point out that our system would be stable ($m > n^2$) only for extremely thin layers of water (< 84 µm for a 1 mm thick lens). For finite-amplitude disturbances, nonlinear effects lead to growth and possibly overturning of interfacial waves (Blyth & Pozrikidis 2004). Our observations indicate that such waves impinge on the lens edge and sometimes break through, prompting the release of surfactant onto the free surface. Finally, we note that the momentum carried by the waves will be enhanced by the viscous boundary layer in the underlying water, thereby facilitating the transfer of surfactant across the lens edge (Frenkel & Halpern 2005).

5. Discussion

We have proposed a consistent physical picture for the oscillations of the sessile lens. One expects a surfactant-laden oil drop placed on a water surface to spread as the tension at the oil–water interface decreases due to adsorbtion of surfactant onto the drop surface. One further expects that the evaporation of surfactant from the air–water surface will also lead to drop expansion. The most puzzling feature of the system is thus the sudden drop retraction. We have observed that the retraction is accompanied by discrete flushing events in which surfactant-coated oil droplets are ejected onto the free surface. We have further observed that these flushing events are coincident with the arrival of interfacial waves at the drop edge. The existence of interfacial waves in our system is consistent with the theoretical predictions of Frenkel & Halpern (2002) for a surfactant-laden interface in the presence of shear. To the best of our knowledge, these experiments provide the first observations of this interfacial instability.

According to the proposed mechanism, differential adsorption generates a Marangoni stress along the lower lens surface, which establishes the observed internal circulation. The latter has two effects. First, it advects surfactant radially outward along the oil–water interface. Second, it provides the non-zero shear condition that, together with the presence of surfactant, renders the oil–water interface unstable to capillary waves (Frenkel & Halpern 2002). The incidence of these waves on the drop edge is observed to coincide with the ejection of surfactant onto the water surface. This ejection process is itself complex, being characterized by the intrusion of a sheet onto the free surface, and the subsequent rupture of this sheet into tendrils and then the pinch-off of these tendrils into the aphrons identified by Sebba (1979). Finally, evaporation of Tergitol from the water surface is critical in preventing saturation of the water surface with surfactant, which would ultimately suppress the oscillations, and in prescribing the frequency of oscillation. No beating was observed when Tergitol was replaced by dodecanol, presumably owing to the different reaction kinetics (rates of adsorption and evaporation) in the oil–dodecanol system.

It is instructive to discuss our mechanism in the light of previous studies of related spontaneous oscillations. Unlike the surfactants used in the systems studied by Dupeyrat & Nakache (1978), Yoshikawa & Matsubara (1983) and Shioi *et al.* (2002), Tergitol is non-ionic, from which one may conclude that the effect of electric charge is negligible in our system. While the precise mechanism responsible for the ejection of surfactant in the spitting drop problem (Fernandez & Homsy 2004; Krechetnikov & Homsy 2004) remains elusive, the authors point out that at the point of pinch-off, the system looks locally like the extended end of a drop in a straining flow such as may be generated by a four-roll mill (Taylor 1934). When the ratio of drop viscosity to suspending fluid viscosity is small, the capillary number sufficiently large, and the drop surface contaminated by surfactant, one anticipates the ejection of droplets from the tip (De Bruijn 1993). We note that such tip streaming cannot be used to rationalize the flushing events observed in our system, where the ratio of the viscosities of the drop and suspending fluid is large.

The oscillation of the sessile lens is remarkable in that it is an example of spontaneous, periodic, partial emulsification. Indeed, this oscillation may be viewed as an intermediary between a static sessile lens and a lens that erupts and vanishes by way of spontaneous emulsification (McBain & Woo 1937). According to our physical picture, the differential adsorption of surfactant onto the lower drop surface generates a Marangoni flow that renders the drop unstable to transverse waves whose arrival at the drop edge prompts emulsification in the form of ejection of surfactant onto the

free surface. The criterion for emulsification in such a system is thus not based entirely on the system chemistry, but also on its dynamics, which will depend specifically on the geometry and fluid properties of the drop, as well as the dependence of surface tension on surfactant concentration. In particular, the vigour of the corner circulation will depend on the shape of the drop, the drop viscosity and the driving Marangoni stress.

There is strong interest in understanding biological oscillators, which underlie many of the mechanisms responsible for life. Biological oscillators are often rationalized in terms of membrane potential oscillations (e.g. nerve and cardiac cells) or, according to more recent models, oscillations of non-electrical nature that arise at the cellular level from the regulation of enzyme, receptor or gene activity (Goldbeter 1996). Conversion of chemical to kinetic energy is often at the heart of the generation of rhythmic movements, expressed in a wide range of animal behaviours including flying, walking, swimming, eating, and visceral processes (Friesen, Block & Hocker 1993). Models for these oscillations have grown increasingly complex, reflecting the complexities underlying the oscillators themselves. The oscillations we describe are a peculiar manifestation of spontaneous and sustained conversion of chemical to kinetic energy, achieved in an exceedingly simple system. While much of the mystery of biological oscillators lies in the complex underlying dynamics of molecular and cellular mechanisms, awareness of simple physico-chemical analogues like the spontaneous oscillations of a sessile lens might prove helpful in modelling some biological oscillators.

REFERENCES

BLYTH, M. G. & POZRIKIDIS, C. 2004 Effect of surfactant on the stability of two-layer channel flow. *J. Fluid Mech.* **505**, 59–86.

DE BRUIJN, R. A. 1993 Tip-streaming of drops in simple shear flows. *Chem. Engng Sci.* **48**, 277–284.

DUPEYRAT, M. & NAKACHE, E. 1978 Direct conversion of chemical energy into mechanical energy at oil water interface. *Bioelectrochem. Bioenergetics* **5**, 134–141.

FERNANDEZ, J. M. & HOMSY, G. M. 2004 Chemical reaction-driven tip-streaming phenomena in a pendant drop. *Phys. Fluids* **16**, 2548–2555.

FODA, M. & COX, R. G. 1980 The spreading of thin liquid films on a water-air interface. *J. Fluid Mech.* **101**, 33–51.

FRANKLIN, B. 1774 Of the stilling of waves by means of oil. *Phil. Trans.* **64**, 445.

FRENKEL, A. L. & HALPERN, D. 2002 Stokes-flow instability due to interfacial surfactant. *Phys. Fluids* **14**, L45–L48.

FRENKEL, A. L. & HALPERN, D. 2005 Effect of inertia on the insoluble-surfactant instability of shear flow. *Phys. Rev.* E **71**, 016302.

FRIESEN, W. O., BLOCK, G. D. & HOCKER, C. G. 1993 Formal approaches to understanding biological oscillators. *Annu. Rev. Physiol.* **55**, 661–681.

GOLDBETER, A. 1996 *Biochemical Oscillations and Cellular Rhythms: The Molecular Bases of Periodic and Chaotic Behaviour*. Cambridge University Press.

HALPERN, D. & FRENKEL, A. L. 2003 Destabilization of a creeping flow by interfacial surfactant: linear theory extended to all wavenumbers. *J. Fluid Mech.* **485**, 191–220.

KOVALCHUK, V. I., KAMUSEWITZ, H., VOLLHARDT, D. & KOVALCHUK, V. I. 1999 Auto-oscillations of surface tension. *Phys. Rev.* E **60**, 2029–2036.

KRECHETNIKOV, R. & HOMSY, G. M. 2004 On physical mechanisms in chemical reaction-driven tip-streaming. *Phys. Fluids* **16**, 2556–2566.

MCBAIN, J. W. & WOO, T. 1937 Spontaneous emulsification, and reactions overshooting equilibrium. *Proc. R. Soc. Lond.* A **163**, 182–188.

MIKSIS, M. J. & VANDEN-BROECK, J. 2001 Motion of a triple junction. *J. Fluid Mech.* **437**, 385–394.

MITCHELL, D. J., TIDDY, G. J. T., WARING, L., BOSTOCK, T. & MCDONALD, M. P. 1983 Phase behaviour of polyoxyehtylene surfactants with water. *J. Chem. Soc., Faraday Trans.* I **79**, 975–1000.

PUJADO, P. R. & SCRIVEN, L. E. 1972 Sessile lenticular configurations: translationally and rotationally symmetric lenses. *J. Colloid Interface Sci.* **40**, 82–98.

SCRIVEN, L. E. & STERNLING, C. V. 1960 The Marangoni effects. *Nature* **187**, 186–188.

SEBBA, F. 1975 Macrocluster gas-liquid an biliquid foams and their biological significance. *A.C.S. Symposium Series* **9**, 18–39.

SEBBA, F. 1979 A surface-chemical basis for cell motility. *J. Theor. Biol.* **78**, 375–391.

SEBBA, F. & BRISCOE, H. V. A. 1940 The variation of the solubility of unimolecular films with surface pressure, and its effect on the measurement of true surface pressure. *J. Chem. Soc.* 114–118.

SHIOI, A., KUMAGAI, H., SUGIURA, Y. & KITAYAMA, Y. 2002 Oscillation of interfacial tension and spontaneous interfacial flow at a water/oil interface composed of Di(2-ethylhexyl) phosphoric acid. *Langmuir* **18**, 5516–5522.

SMITH, M. K. & DAVIS, S. H. 1983 Instabilities of dynamic thermocapillary liquid layers. Part 1. Convective instabilities. *J. Fluid Mech.* **132**, 119–144.

TAYLOR, G. I. 1934 The formation of emulsions in definable fields of flow. *Proc. R. Soc. Lond.* A **146**, 501–523.

YOSHIKAWA, K. & MATSUBARA, Y. 1983 Spontaneous oscillation of pH and electrical potential in an oil–water system. *J. Am. Chem. Soc.* **105**, 5967–5969.